# Image correlation analysis를 이용한 종이의 재료 역학적 특성에 관한 연구 II

임 기 증 · R. W. Perkins* · 김 형 진**
강원대학교 창강제지기술연구소
* Professor Emeritus, Dept. of Mechanical, Aerospace and Manufacturing Engineering, Syracuse University, USA
** 국민대학교 임산가공학과

## 1. Introduction

Consideration of the stress and strain solution in the vicinity of a hole in a plate has been the subject of numerous papers involving metals, composites, wood and paper [1-9]. The presence of the hole causes the stress and strain components to be much higher than would be the case without the hole. Consequently, failure of the plate resulting from high loads will be initiated at the edge of the hole. The principal issue is the problem of how to best model the state of stress and strain in a situation where the solution varies through the plane of the structure. In the case of a brittle material, the solution can be achieved through the theory of linear elasticity. For a material such as paper, the elasticity solution is not appropriate when the load approaches the failure value since paper behaves in a strongly nonlinear manner. As a result of the complex nonlinear material behavior, the solutions of problems of this type are often sought using the finite element method. The finite element method permits the solution to problems with spatially varying solutions involving complex geometry and complex material behavior.

Overall objective of this study is to investigate how paper behaves when in-plane loading is high enough for non-linear effects. Strain components around the circular hole (especially along lines leading from the hole edge along the longitudinal and lateral axes), will be obtained using image correlation analysis at several load levels to provide a data set

for finite element analysis.

## 2. Material and method

### 2.1 Material

The paper material selected for this study is a greeting card paper. This paper has a basis weight of 122 $g/m^2$, a density of approximately 676 $kg/m^3$, and exhibits a strongly anisotropic and nonlinear behavior. Liner has been also used for measuring the nature and extent of damage that takes place around the hole preceding failure.

### 2.2 Digital camcorder

A SONY DCR-TRV 730 digital video camera recorder was used to acquire digital images of the surfaces of undeformed and deformed paper specimens. The use of the digital camcorder is advantageous, since it eliminates the need for a frame grabber option that converts the camera signal from analog to digital form for computer processing. In practice, the digitizing process can cause the gray-value at any pixel to vary from image to image as the frame grabber converts the camera signal from analog to digital form.

### 2.3 Image correlation software

VIC_2D (Beta 3.0.3 version) image acquisition software developed at the University of South Carolina was used. The digital camcorder was set up approximately 152.4 cm from the specimen in order to compensate for any "out of plane motion" of the specimen. This gave a field of view of approximately 4 square inches at the maximum zoom-in of the digital camcorder. A standard photographic tripod was used for a camera mount in this research. Special care was taken to ensure that the image plane of the camera was exactly parallel with the test specimen surface.

### 2.4 Testing machine

All experiments were carried out using a 50kN capacity Instron Model 4204 electromechanical universal testing machine. This machine is designed for testing materials in

tension, compression, shear, and flexure from 0.1 N to 50 kN. The test machine is composed of loading frame components and control console components. The Model 4204 incorporates a microprocessor controlled, closed-loop, and servo drive system with an optical encoder feedback assuring accurate and constant crosshead speed. Thus speeds are independent of the voltage, frequency, or applied force (with rating).

## 3. Results and Discussions

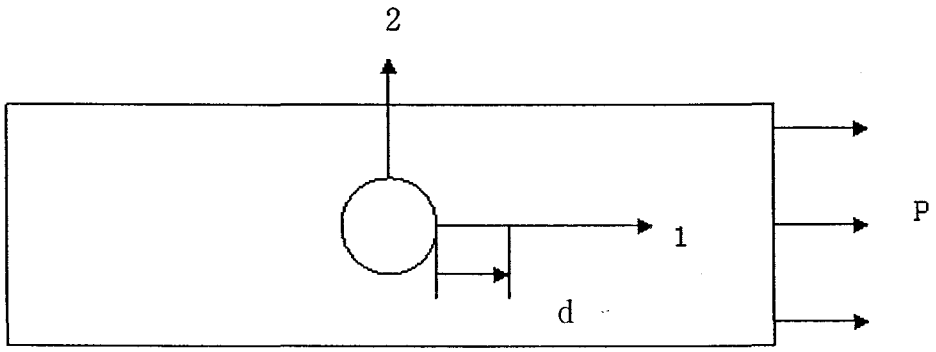


Figure 1. Tensile specimen with central hole.

The mechanics problem consisted of a tensile strip with a central hole as illustrated in Figure 1. The loading was applied at the right edge by displacement control provided by an Instron machine. The left edge was fixed. The hole diameter was 0.635 cm. The sample length was 26 cm. Three specimen widths were studied: 1.6 cm, 4.3 cm and 8.9 cm. Experimental measurement of the strains using an image correlation method was focused on the regions emanating outward from the hole along the 1 and 2 coordinate directions.

Figure 2. Strain component $E_{11}$ along the $x_1$ axis for load level 1. Sample m4. Although there is considerable scatter, the strain appears to have a negative value as the hole edge is approached. As the interior of the sample is reached the strain appears to average to a value of 0.006, which was the value of the nominal applied strain for load

level 1. The scatter in strain value is quite large and the variation from minimum to maximum strain at some distance from the hole is greater than the average value.

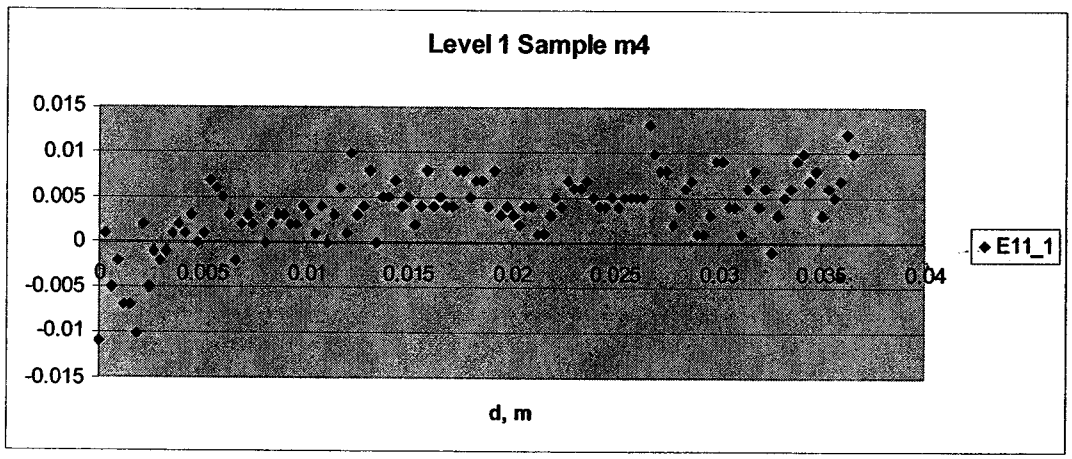


Figure 2. Strain component $E_{11}$ along the $x_1$ axis for load level 1. Sample m4.

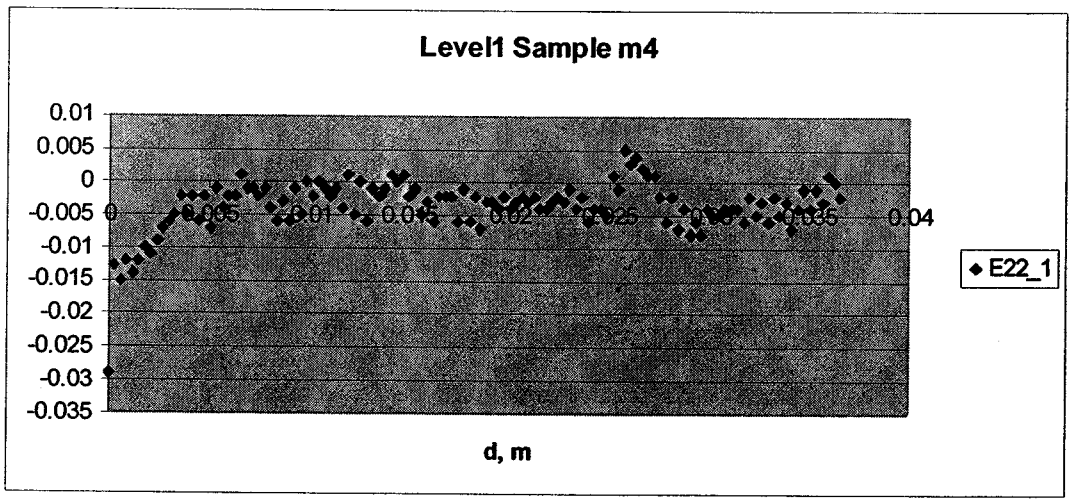


Figure 3. Strain component $E_{22}$ along the $x_1$ axis for load level 1. Sample m4.

Figure 3 illustrates the results for strain component $E_{22}$ along the $x_1$ axis, E22_1. This data appears be exhibit somewhat less scatter. The values clearly become negative as the hole surface is approached. As the distance d from the hole edge increases, the values center on a value slightly below zero. This trend appears to be exactly as expected since as the distance from the hole increases, the strain field should be the same as that for a tensile specimen without a hole.

Consider next the result obtained for strain component $E_{11}$ along the $x_2$ axis illustrated by Figure 4. The data for each step is plotted. Note that step 4 represents essentially the recovery strain following the unloading step. Figure 5 shows the same data where the data are summed to give the results for the 4 load levels. Note that the result for level 4 represents the field of residual strain. It can be concluded that there is extensive nonrecoverable strain remaining in the vicinity of the hole after load removal.

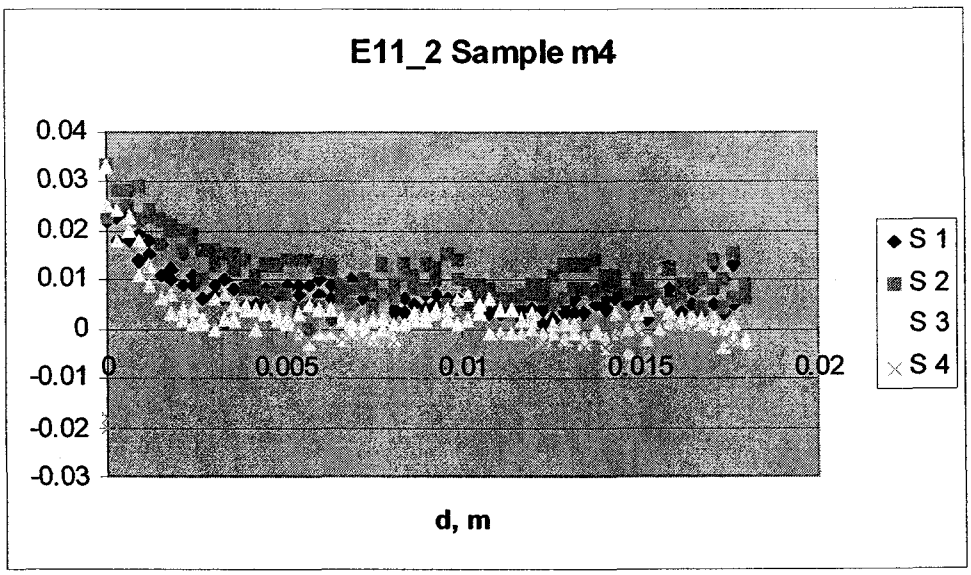


Figure 4. Strain component $E_{11}$ along the $x_2$ axis. Results are shown for each of the 4 load steps.

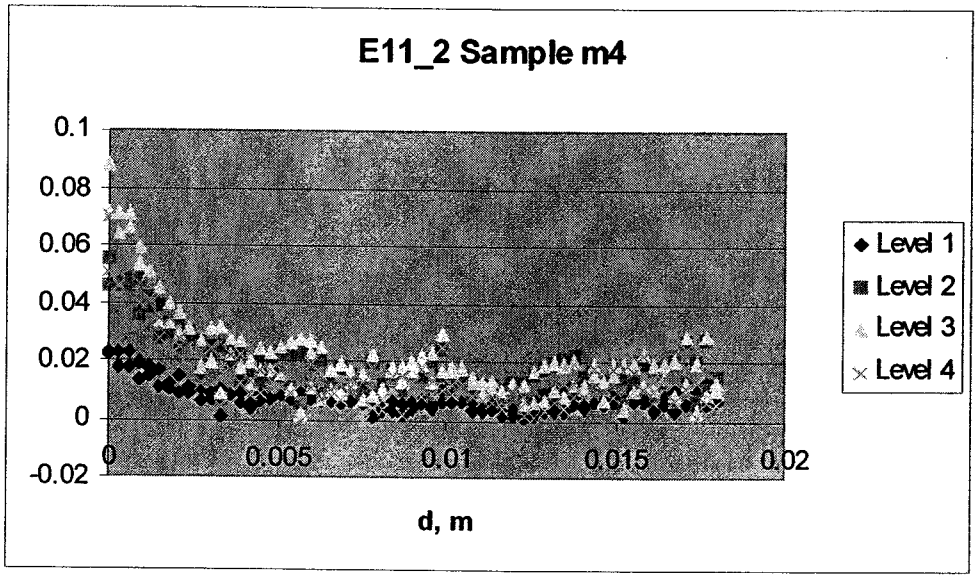


Figure 5. Strain component $E_{11}$ along the $x_2$ axis corresponding to the 4 load levels.

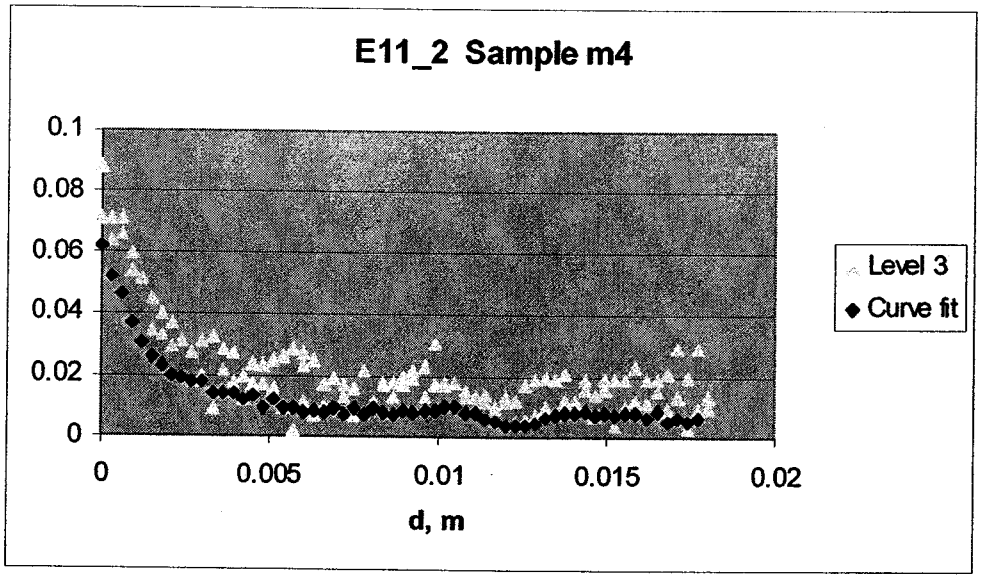


Figure 6. Strain component $E_{11}$ along the $x_2$ axis. Comparison of gradient data and data obtained after curve-fitting the displacement curve.

In Figure 6 we compare the gradient data taken directly from the image processing output and compare the strain computed by fitting a straight line to the $u_1$ displacement data in the 7 lines emanating from the hole in the direction of the $x_2$ axis. It is of interest to note that the curve-fitting method removes a great deal of scatter, however, it appears that the resulting strain values are consistently lower than those obtained directly from the displacement gradient data. It does not appear to be clear which of the two representations is the more correct. A similar finding was obtained in the case of strain $E_{22}$ along the $x_2$ axis. See Figure 7.

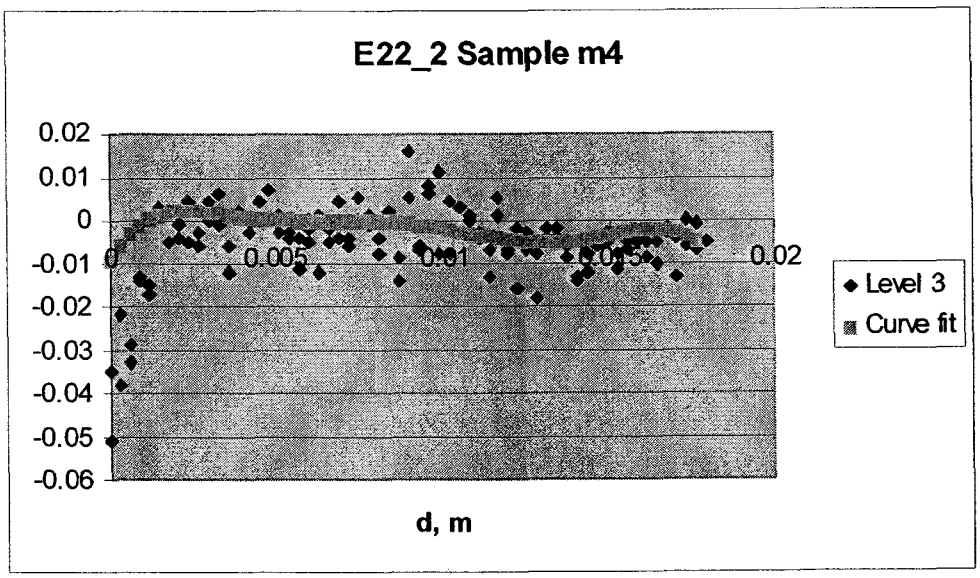


Figure 7. Strain component $E_{22}$ along the $x_2$ axis. Gradient data compared with strain calculated by a curve-fitting method.

Here also it is clear that the curve-fitting method seemsto remove a lot of the scatter, however, again it is not clear which representation of the strain is the more correct. A problem that can easily occur with a curve-fitting method is that the trends at the

extremes of the data may not be very good. Thus, it is not clear that the curve-fitting method is better for computing the strain values.

## 4. Conclusion

The results show that the strains in the vicinity of the hole are very nonlinear. This is particularly apparent from a study of the strain component $E_{11}$ along the $x_2$ axis as illustrated by Figure 5. At the hole edge, the residual strain is on the order of 7 percent. The highest strain, which occurs at load level 3, is about 9 percent. Based on the tensile strength property tests, the failure strain under uniform stress conditions is approximately 2 percent. It seems likely that failure has actually occurred at this point in the specimen. Failure can be expected to occur as a localized failure. Crack propagation and total fracture may be prevented by the field conditions further away from the hole surface. If a localized failure has taken place, the disruption of the paper fiber network may have led to problems in image processing. It would be of considerable interest to explorethe physics of a localized disruption in the network in those zones of very high strain. Further research needs to be initiated with this objective.

## 5. References


1. Daniel, I.M., Rowlands R.E., and Post, D., *Experimental mechanics*, 246-252 (June 1973)

2. Tan, S.C. and Kim, R. Y., *Experimental mechanics*, 345-351 (December 1990)

3. Kortshot, M.T. and Trakas, K., *Tappi J.* 81(1):254-259 (1998)

4. Rowlands, R.E., Daniel, I. M, and Whiteside, J. B., *Experimental mechanics*, 31-37 (January 1973)

5. Daniel, I.M. and Rowlands, R.E., *J. Composite Materials* 5:250-254 (April 1971)

6. Merrill, P. S., *Experimental mechanics*, 73-80 (August 1961)

7. Ko, W. L., "Stress Concentration Around a Small Circular Hole in the HiMAT Composite Plate", NASA Technical Memorandum 86038 (1985)

8. Whitney, J. M. and Nuismer, R. J., *J. Composite Materials* 8:253-265 (July 1974)

9. Tan, S. C., *J. Composite Materials* 22:1080-1097 (November 1988)

10. Bronkhorst, C. A. and Bennett, K. A., 2002. Deformation and Failure Behavior of Paper. Handbook of Physical Testing of Paper, Second Edition. R. E. Mark, C. C. Habeger, J. Borsch and M. B. Lyne, Marcel Dekker, Vol. I, pp. 313-428.